ТЕРМОДИНАМІЧНИЙ АНАЛІЗ ТА МОДЕЛЮВАННЯ

УДК 532.542.3+532.517.3+532.527.2

The wave model of secondary flows and coherent structures in pipes

S. Surkov✉
Odessa National Polytechnic University, 1 Shevchenko av., Odessa, 65044, Ukraine
✉ e-mail:: ssv@opu.ua
ORCID: https://orcid.org/0000-0002-3112-3041

In this article, a theoretical analysis of the flows arising in the cross sections of fluid and gas flows is performed. Such flows are subdivided into secondary flows and coherent structures. From experimental studies it is known that both types of flows are long-lived large-scale movements (LSM) stretched along the flow. The relative stability of the vortices is traditionally explained by the fact that the viscous friction forces that inhibit the rotation are compensated by the intensification of the swirl when moving slowly rotating peripheral layers to the center of the vortex due to longitudinal tension. An analysis of this mechanism made it possible to develop a relatively simple model of vortex structures in which the viscous friction forces and axial expansion are considered to be infinitesimal. Under these assumptions, one can use the equations of motion of an ideal fluid in the variables "stream function - vorticity". It is shown that under certain assumptions these equations take the form of a wave equation, and the boundary conditions are the condition that the stream function on the solid walls of the flow equals zero. The obtained solutions of the wave equation describe the following special cases: Goertler's vortices between rotating cylinders, secondary flows in a pipe with a square cross section, swirling flow in a round pipe, paired vortex after bend of the pipe. The physical sense of more complex solutions of the wave equation has become clear relatively recently. Very similar structures were found in experimental studies using orthogonal decomposition (POD) of a turbulent pulsations field. This may mean that the eigenfunctions in the POD correspond to coherent structures that really arise in the flow. The results obtained confirm the hypothesis that secondary flows and coherent structures have a common nature. The solutions obtained in this paper can be used in processing the experiment as eigenfunctions for the orthogonal decomposition method. In addition, they can be used in direct numerical simulation (DNS) of turbulent flows.

Keywords: *Secondary flows; VLSM; Coherent structures; Orthogonal decomposition method; Eigenfunctions.*

doi: https://doi.org/10.15673/ret.v55i5-6.1655

1. Introduction

The study of the structure of turbulent flows is one of the most important problems of fluid mechanics. Many semi-empirical turbulence models have been developed, but all of them have limited applications. In significant cases, the results of computer simulation of fluid and gas flows ought to be verified by experiment. Rational turbulence models can not only increase the accuracy of modeling, but also essentially accelerate the calculation process.

Understanding the structure of turbulent flows can help in finding ways to reduce hydraulic resistance, or to intensify heat and mass transfer in technological equipment.

Turbulence models are important in calculating two-phase flows. In liquid-vapor systems, they allow one to determine the areas of appearance and collapse of bubbles. In systems "gas-solid particles" they help to predict the speed and zone of deposition of dust particles.

A number of studies prove the close relationship

between secondary flows and coherent structures. The transition to turbulence can begin with the uprise of secondary flows, continue as the formation of increasingly complex coherent structures, and finally, lead to the appearance of developed turbulence, where it is difficult to distinguish ordered structures.

Enhancement of the theoretical models of secondary flows and coherent structures seems to be an urgent task.

2. Literature Review

Secondary flows were discovered experimentally and described in [1]. The essence of the phenomenon is that if the main flow moves parallel to the *x* axis, then flows with closed streamlines (eddies) arise in the cross section *yOz*, the dimensions and shape of which are determined by the boundary conditions.

According to the Prandtl classification, secondary flows of the first kind arise in the cross sections of pipes or channels under the action of mass forces [2]. Their classic example is the twin vortex that arises in a bent round tube under the influence of centrifugal force.

Secondary flows of the second kind arise in the channels of a non-circular cross section, apparently due to the uneven distribution of the shear stresses on the wall. Secondary flows of the third kind arise near bodies oscillating.

Structures that have many features in common with secondary flows arise in a number of cases in the process of transition from the laminar mode of motion to turbulent one. Some of the most characteristic examples are Taylor vortices between rotating cylinders and Goertler vortices on a curved surface [3].

The classical model of a stationary vortex is known, the attenuation of which, due to the forces of viscous friction, is compensated by the intensification of the swirl associated with the extension of the vortex along the axis [4]. This analysis allowed to suggest that if we neglect simultaneously the forces of viscous friction and the axial extension of the vortex, then we can obtain a rather simple but close to reality model of secondary flows [5, 6].

Simplified theoretical models of secondary flows arising in the channels of prismatic [5] and circular [6] cross sections are obtained. The streamlines and secondary current velocities are calculated. In [6], it was suggested that the obtained models of secondary flows can arise in pipes during the transition from the laminar flow regime to the turbulent one. But in 2003, there was no experimental evidence for this assumption.

In recent years, in experimental studies of turbulent flows, significant progress has been achieved associated with the use of the sPIV method – stereoscopic particle image velocimetry [7, 8]. The essence of the method is that a lot of hollow glass balls with a size of about 10 μm are added to the turbulent flow. The average density of the balls is almost equal to the density of the liquid, which provides neutral buoyancy. Using high-resolution cameras, images of the flow are obtained, which, using computer processing, make it possible to obtain a three-dimensional field of instantaneous fluid velocities in the cross section being studied.

Next, the search for coherent structures war performed by the method of snapshot proper orthogonal decomposition (POD). The large-scale motions (LSM) and very large-scale (VLSM) motions were distinguished. It was noted that these motions are closely related to secondary flows, as well as to coherent structures that occur during the transition to turbulence [9].

According to the results of the POD analysis, the most energy-efficient coherent structures were synthesized. Fluctuations in the longitudinal velocity and streamline of the secondary flows in the cross section were visually presented in [10-12].

This article shows that secondary flows and large-scale coherent structures, distinguished by processing the experimental data, are in good agreement with the wave model developed by us.

3. Equations describing secondary flows

Most secondary flows are long-lived vortices, elongated in the direction of the main stream.

Let us consider a steady flow in a channel stabilized along the *x* axis. This means that the flow rates do not change along the *x* axis, but only pressure changes due to irreversible loss of potential energy. In this case, the Navier-Stokes equations are written in the form

$$u_y \frac{\partial u_x}{\partial y} + u_z \frac{\partial u_x}{\partial z} = X - \frac{1}{\rho}\frac{\partial p}{\partial x} + \nu\left(\frac{\partial^2 u_x}{\partial y^2} + \frac{\partial^2 u_x}{\partial z^2}\right); \quad (1)$$

$$u_y \frac{\partial u_y}{\partial y} + u_z \frac{\partial u_y}{\partial z} = Y - \frac{1}{\rho}\frac{\partial p}{\partial y} + \nu\left(\frac{\partial^2 u_y}{\partial y^2} + \frac{\partial^2 u_y}{\partial z^2}\right); \quad (2)$$

$$u_y \frac{\partial u_z}{\partial y} + u_z \frac{\partial u_z}{\partial z} = Z - \frac{1}{\rho}\frac{\partial p}{\partial z} + \nu\left(\frac{\partial^2 u_z}{\partial y^2} + \frac{\partial^2 u_z}{\partial z^2}\right). \quad (3)$$

This system of equations is closed by the continuity equation

$$\frac{\partial u_y}{\partial y}+\frac{\partial u_z}{\partial z}=0.. \qquad (4)$$

Equation (4) allows using the stream function ψ in the cross section of the flow, while the continuity equation is automatically satisfied [3, 4].

If we consider the flow as two-dimensional (flat), then only the projection of the vorticity of the flow onto the *x* axis makes sense:

$$\Omega=\frac{\partial u_z}{\partial y}-\frac{\partial u_y}{\partial z}.$$

Since $u_y=\frac{\partial\psi}{\partial z}$ and $u_z=-\frac{\partial\psi}{\partial y}$, we can write

$$\Omega=-\frac{\partial^2\psi}{\partial y^2}-\frac{\partial^2\psi}{\partial z^2}=-\nabla^2\psi. \qquad (5)$$

We consider mass forces to be potential. Differentiating equation (3) with respect to *y*, and (2) with respect to *z*, and subtracting the results, we obtain

$$u_y\frac{\partial\Omega}{\partial y}+u_z\frac{\partial\Omega}{\partial z}=\nu\left(\frac{\partial^2\Omega}{\partial y^2}+\frac{\partial^2\Omega}{\partial z^2}\right). \qquad (6)$$

In view of (5), we obtain the equation in the variables "stream function – vorticity":

$$\frac{\partial\psi}{\partial z}\frac{\partial\Omega}{\partial y}-\frac{\partial\psi}{\partial y}\frac{\partial\Omega}{\partial z}=\nu\left(\frac{\partial^2\Omega}{\partial y^2}+\frac{\partial^2\Omega}{\partial z^2}\right). \qquad (7)$$

And finally, neglecting the viscosity, we obtain:

$$\frac{\partial\psi}{\partial z}\frac{\partial\Omega}{\partial y}-\frac{\partial\psi}{\partial y}\frac{\partial\Omega}{\partial z}=0. \qquad (8)$$

On the left side of equation (8) is the functional determinant (Jacobian) of the functions ψ and Ω. The equality of this determinant to zero means that between ψ and Ω there is a functional dependence independent of the coordinates *y* and *z*.

To get specific solutions, suppose this relationship is linear:

$$\Omega=C\psi,$$

where *C* is a constant.

Thus, there is a subset of solutions of equation (8) that satisfy the equation

$$\nabla^2\psi=C\psi. \qquad (9)$$

Equation (9) is known in mathematical physics as the Helmholtz equation, the Mathieu-Weber equation, or the plane wave equation. It describes standing waves of various nature, for example, membrane vibrations, an electron in a potential well, etc.

Below we consider some solutions of equation (9) and find out their hydromechanical sense.

4. Results and Discussions

4.1. Secondary flows in prismatic channels

Equation (9) in Cartesian coordinates takes the form

$$\frac{\partial^2\psi}{\partial y^2}+\frac{\partial^2\psi}{\partial z^2}=C\psi. \qquad (10)$$

Its solution in the general case is the sum of sinusoidal functions. Since, using trigonometric transformations, the sum of sinusoidal functions can always be represented as a product, the solutions of equation (10) can be written as

$$\psi=A\prod_{i=1}^{n}\sin k_i\xi_i, \qquad (11)$$

where ξ_i are the auxiliary axes in the $y_\theta(z)$ plane; k_i – wave numbers.

The solutions of equation (10) corresponding to specific boundary conditions were obtained as follows. Initially, several auxiliary axes were drawn perpendicular to the channel walls, herewith

$$\xi_i=y\cos\varepsilon+z\sin\varepsilon, \qquad (12)$$

where ε is the angle between the auxiliary axis ξ_i and the *y* axis.

At the boundaries of the vortex cells, the vorticity always equals zero [5, 6]. Therefore, the directions of the ξ_i axes and the wave numbers k_i were chosen so that at the boundaries of the cells, and, in particular, on the channel walls, one of the factors in expression (11) was equal zero: $\sin \xi_i k_i = 0$. The structure of expressions (11) was checked using computer visualization.

4.1.1. Mathematical Model of Taylor Vortices

This flow is described by a stream function

$$\psi=A\sin k_1 y\sin k_2 z. \qquad (13)$$

The surface described by the equation (13) is shown as a three-dimensional graph in Fig.1. The streamlines of the secondary flow are obtained as horizontal slices of this surface.

The streamlines ψ=const for this flow are plotted in Fig. 2 using the universal algorithm described in [13]. During the plotting, the value ψ was changed with a constant step Δψ.

In the case under consideration, projections of the

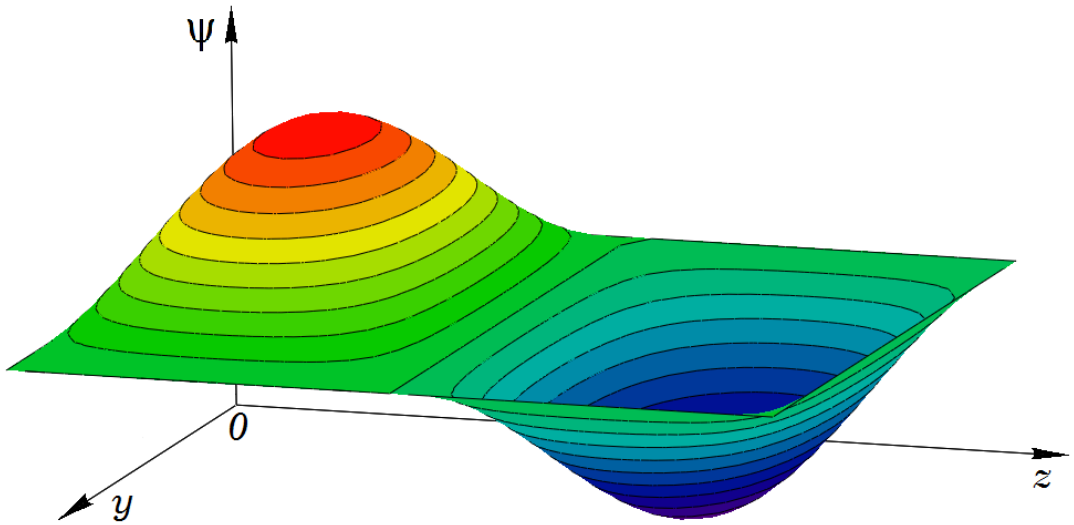

Figure 1 *– The surface described by the equation (13) and the principle of plotting of the streamlines*

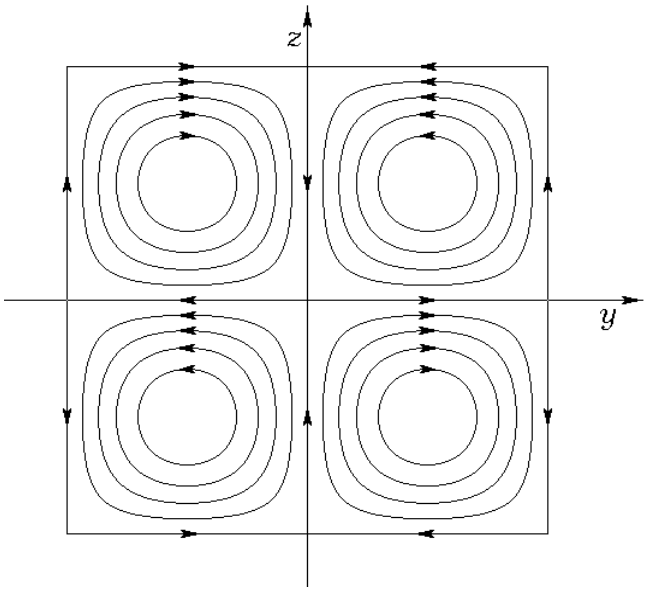

Figure 2 *– The streamlines described by equation (13), plotted with a step Δψ = 0,2*

flow velocity are

$$u_y = Ak_2 \sin k_1 y \cos k_2 z,$$

$$u_z = -Ak_1 \cos k_1 y \sin k_2 z.$$

Analyzing Fig. 2, we can conclude:

a) a common vertex can belong only to an even number of cells, because vortices having a common boundary should rotate in opposite directions;

b) the total number of vortices in the flow must be even by virtue of the law of conservation of angular momentum.

If one row of vortices is selected in the resulting flow pattern, then the similarity with the cross section of Taylor vortices between rotating cylinders [3] shown in Fig. 3.

In our opinion, similar structures in narrow channels of rectangular cross section were also observed in experimental works [14, 15].

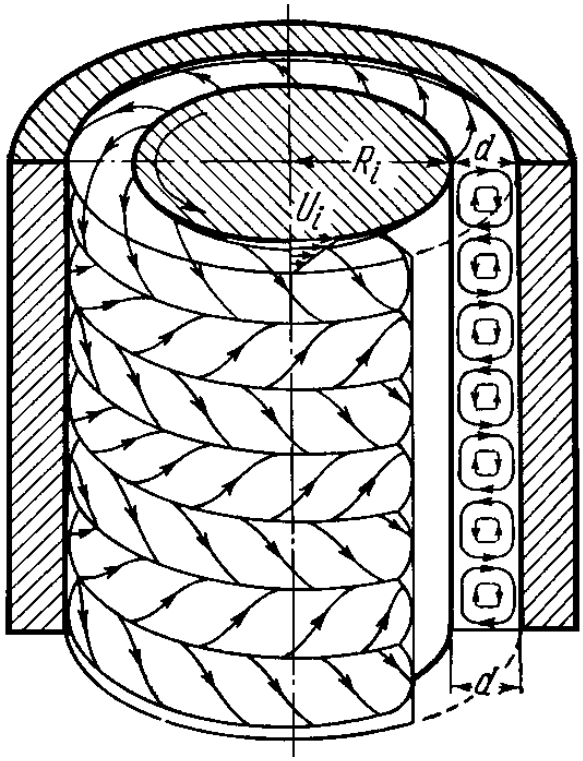

Figure 3 *– Taylor vortices between rotating cylinders according to [3]*

4.1.2. Secondary flow model in a square cross-section pipe

This flow is described by a stream function.

$$\bar{\psi} = \sin \bar{y} \sin \bar{z} \frac{\bar{z} + \bar{y}}{2} \sin \frac{\bar{z} - \bar{y}}{2}.. \qquad (14)$$

The streamlines for this flow are shown in Fig. 4. Comparing these streamlines with the data of

other authors [16], a significant similarity can be noted.

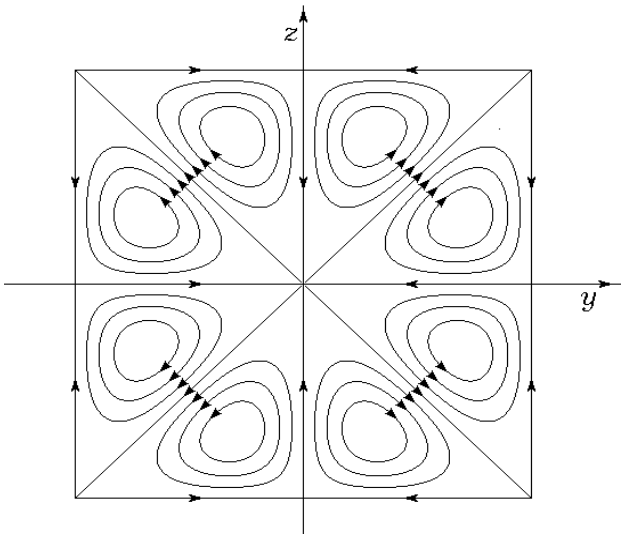

***Figure 4** – The streamlines of the flow described by equation (14) at Δψ = 0,1*

4.2. Secondary flows in round pipes

The equation (9) written in polar coordinates (r, Θ) is:

$$\frac{\partial^2\psi}{\partial r^2}+\frac{1}{r}\frac{\partial\psi}{\partial r}+\frac{1}{r^2}\frac{\partial^2\psi}{\partial\theta^2}=k^2\psi, \qquad (15)$$

where k^2 is a constant.

Equation (23) is solved by separating the variables [17]:

$$\psi(r,\theta)=f_1(r)\,f_2(\theta),$$

where

$$f_1(\bar{r})=C_1J_m(r)+C_2N_m(r)+C_3I_m(r)+C_4K_m(r), \qquad (16)$$
$$f_2(\theta)=\sin(m\theta+\theta_0),$$

where $J_m(r)$ are the Bessel functions of the first kind; $N_m(r)$ – Neumann functions (Bessel functions of the second kind); $I_m(r)$ and $K_m(r)$ – Bessel functions of a complex argument (modified Bessel functions); C_1, C_2, C_3, C_4 are constants.

All the functions included in (16), except $J_m(r)$, have infinite values at $r = 0$. Since infinite values of ψ do not have physical sense, only the first term remains in solution (27). Thus, the final decision has the form

$$\psi=C_1J_m(r)\sin(m\theta+\theta_0), \qquad (17)$$

where C_1 is the amplitude value of the current function, m^2/s; θ_0 – starting angle, rad.

In relative variables, expression (17) takes the form

$$\bar{\psi}=J_m(\bar{r})\sin(m\theta).. \qquad (18)$$

where $\bar{\psi}=\psi/C_1$.

The dimensionless radius may be chosen as

$$\bar{r}=\frac{r}{R}j_{m,n},$$

where $j_{m,n}$ are the roots of the function $J_m(r)$.

With this normalization, the pipe walls will always coincide with the boundaries of the vortex cells, where $\bar{\psi}=0$, and at the radius of the pipe n vortex cells will be stacked.

In the course of hydromechanical analysis of solutions (18), for different values of m and n, streamlines were plotted and the projections of the fluid velocity were determined:

$$u_r=\frac{1}{r}\frac{\partial\psi}{\partial\theta}; \qquad (19)$$

$$u_\theta=-\frac{\partial\psi}{\partial r}. \qquad (20)$$

Let us consider particular cases of solutions described by equation (18) and plot the streamlines.

4.2.1. Model of a twin vortex arising in a bent pipe

This flow is described by the stream function (18) at $n = 0$. The stream function takes the form

$$\bar{\psi}=J_1(\bar{r})\sin\theta. \qquad (21)$$

From (19) and (20) the projection of the fluid velocity are

$$\bar{u}_r=\frac{1}{\bar{r}}J_1(\bar{r})\cos\theta,$$

$$\bar{u}_\Theta=\left[\frac{1}{\bar{r}}J_1(\bar{r})-J_0(\bar{r})\right]\sin\theta.$$

The tangential velocity $u_\theta(z)$ on the z axis coincides with u_y. The stream lines and velocities for this case are presented in Fig. 5.

Fig. 5 shows that the resulting flow can be considered as a model of a twin vortex arising in a bent pipe. Like other cases, the stream function turns to zero on the pipe walls. However, the azimuthal velocities of the liquid on the walls aren't equal zero, which is a common drawback of solutions based on the ideal fluid model.

4.2.2. Models of coherent structures in round pipes

In [5, 6], experimental data corresponding to m>1 and n>1 were not found. However, such data appeared nowadays.

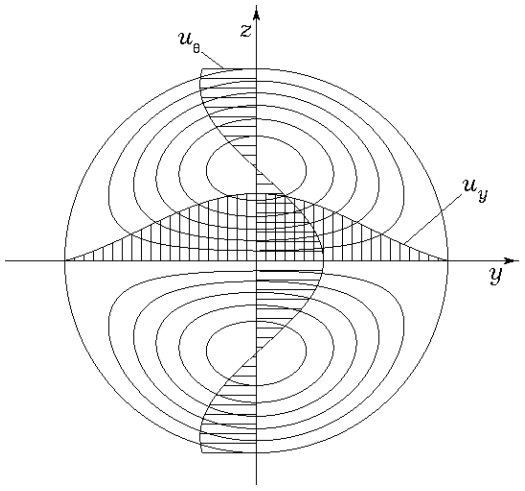

***Figure 5** – The picture of the flow described by equation (18) at m =1 and n =1*

In [7, 8, 12], the structure of turbulent flows in pipes was studied. The sPIV method was used to determine the instantaneous fluid velocities at many points. The obtained experimental values were then "decomposed" into the basic functions using the proper orthogonal decomposition (POD). While the basic functions depending on the angle θ were obviously sinusoids, dozens of functions were summed to describe dependences of the radius *r*.

We want to show that the expansion in radius is much simpler if we use functions of the form (18).

In Fig. 6, the experimental data of the work [7] are compared with the results of calculations by formula (18) at different values of *m* and *n*.

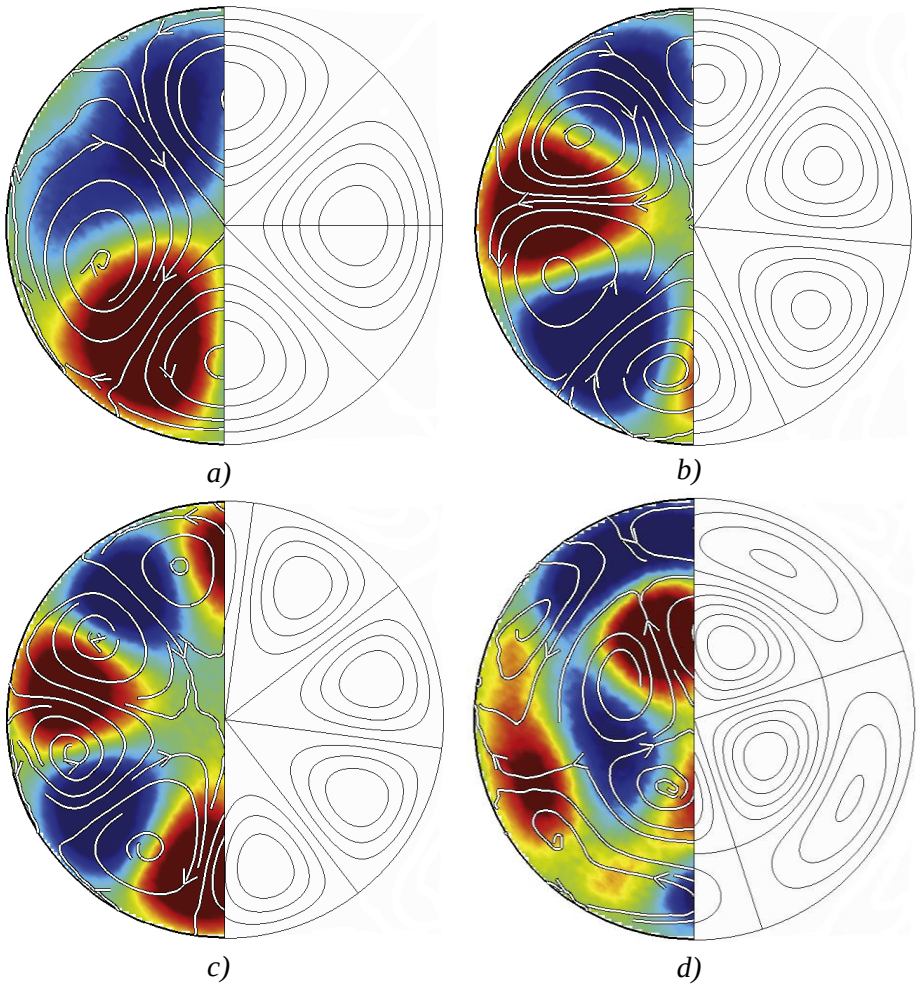

***Figure 6** – Comparison of streamlines calculated according to (18) (right halves) with experimental data [7] (left halves. a) m = 2, n = 1; b) m = 3, n = 1; c) m = 4, n = 1; d) m = 2, n = 2*

In [18], it was noted that the proposed model of secondary flows can be obtained as a special case of swirling flows in which the longitudinal velocity is directly proportional to the vorticity. However, as can be seen from Fig. 6, this contradicts the experimental data [7].

Note the orthogonality property of Bessel functions, which is expressed by the equation

$$\int_0^1 J_m\left(\frac{r}{R} j_{m,n_1}\right) J_m\left(\frac{r}{R} j_{m,n_2}\right) r dr = 0, \quad n_1 \neq n_2$$

Thus functions

$$S(r) = \sqrt{r} J_m\left(\frac{r}{R} j_{m,n}\right). \qquad (22)$$

are orthogonal on the interval (0, 1). Graphs of these functions are presented in Fig. 7.

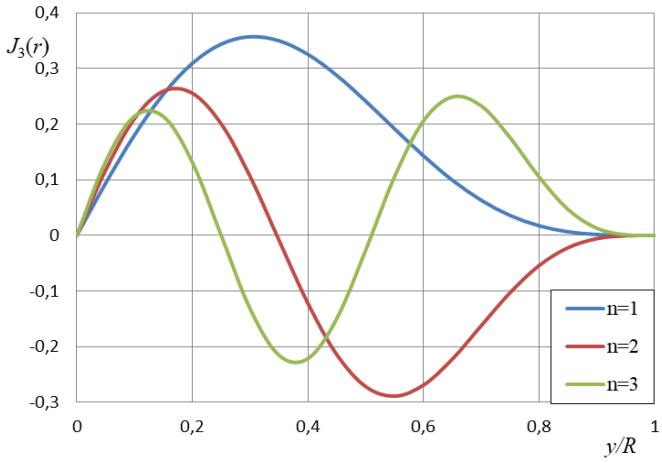

***Figure 7** – Graphs of functions (22) forming an orthogonal basis*

This property shows that this system of functions can be used as a basis for the further development of the method of orthogonal decompositions.

5. Conclusions

This article proposes an approximate theoretical model that considers the structural elements of turbulent flows as vortex waves. This model describes most of the known secondary flows. In addition, the structures predicted using this model are in good agreement with the experimental data obtained in pipes of rectangular and circular cross-section.

The systems of orthogonal functions used in this paper can be applied to improve the methods of orthogonal decompositions, as well as in direct numerical simulation (DNS) of turbulent flows.

References

1. **Nikuradze, J.** (1930) Turbulent flows in non-circular tubes. *Ing.-Archiv, 1, 306-332.*
2. **Prandtl, L.** (1951) Hidroaeromekhanika. *M.: Vydvo inoz. lit., 576.*
3. **Shlikhtinh, H.** (1974) Teoriya pohranychnoho sharu. *M.: Nauka, 712.*
4. **Loycyanskiy, L. H.** (1987) Mekhanika ridyny i hazu. *M.: Nauka, 840.*
5. **Surkov, S. V.** (2002) Khvylova model vtorynnykh techiy v pryzmatychnykh kanalakh. *Tr. Odes. Politekhn. un-tu, 2(18), 184-188.*
6. **Surkov, S. V.** (2003) Vtorynni techiyi v kanalakh z kruhlym i kiltsevym poperechnym pererizom. *Tr. Odes. politekhn. un-tu, 1(19), 14-18*
7. **Hellström, L. H. O., Smits, A.J.** (2014) The energetic motions in turbulent pipe flow. *Phys. Fluids 26, 125102*. DOI: 10.1063/1.4902436
8. **Hellström, L. H. O., Sinha, A., Smits, A.J.** (2011) Visualizing the very-large-scale motions in turbulent pipe flow. *Physics of Fluids, 23, 011703.*
9. **Monty, J. P., Stewart, J. A., Williams, R. C., Chong, M. S.** (2007) Large-scale features in turbulent pipe and channel flows. *Journal of Fluid Mechanics, 589, 147*. DOI: 10.1017/S002211200700777X
10. **Baltzer, J. R., Adrian, R. J., Wu, X.** (2013) Structural organization of large and very large scales in turbulent pipe flow simulation. *Journal of Fluid Mechanics, 720, 236–279.*
11. **Dennis, D., Sogaro, F.** (2014) Distinct organizational states of fully-developed turbulent pipe flow. *Phys. Rev. Lett. 113, 234501.*
12. **Hellström, L. H. O., Ganapathisubramani, B., Smits, A.J.** (2016) Coherent structures in transitional pipe flow. *Physical Review Fluids, 1, 024403.*
13. **Surkov, S. V.** (2004) Kompyuterna vizualizatsiya ploskykh techiy nestyslyvoyi ridyny. *Tr. Odes. Politekhn. un-tu, 1(21), 205-208.*
14. **Arsiriy, E. A., Arsiriy, V. A., Vasilevskaya, A. P.** (2005) Analiz zobrazhen hidrodynamichnykh potokiv za dopomohoyu otsinky parametriv vykhrovykh khvylovykh struktur. *Tr. Odes. Politekhn. un-tu, 1(23), 107–111.*
15. **Arsiriy, V., Kravchenko, O.** (2018) Reconstruction of turbomachines on the basis of the flow structure visual diagnostics. *International Journal of Mechanics and Mechanical Engineering, 22, 2, 405-414.*
16. **Matin, R., Hellström, L. H. O., Hernández-García, A., Mathiesen, J., Smits, A. J.** (2018) Coherent structures in turbulent square duct flow. *International Journal of Heat and Fluid Flow*, 74, 144-153. DOI: 10.1016/j.ijheatfluidflow.2018.08.007.
17. **Korenev, B. H.** (1960) Deyaki zadachi teoriyi pruzhnosti i teploprovidnosti, yaki vyrishuyutsya v beselevykh funktsiyakh. *M .: Fizmathiz, 460.*
18. **Surkov, S. V., Horbatenko, E. A.** (2009) Kinematychni vlastyvosti dvoparametrychnykh vykhrovykh techiy. *Tr. Odes. politekhn. un-tu, 1(31), 139–142.*

Received 27 September 2019
Approved 03 December 2019
Available in Internet 03February 2020.

Хвильова модель вторинних течій і когерентних структур в трубах

С. В. Сурков ✉
Одеський національний політехнічний університет, пр-т Шевченка, 1, м. Одеса, 65044, Україна
✉ e-mail:: ssv@opu.ua
ORCID: https://orcid.org/0000-0002-3112-3041

У статті виконано теоретичний аналіз течій, що виникають в поперечних перетинах потоків рідини і газу. Такі течії поділяються на вторинні течії і когерентні структури. З експериментальних досліджень відомо, що обидва типи течій є довгоживучі великомасштабні вихри, витягнуті уздовж потоку. Відносна стабільність вихорів традиційно пояснюється тим, що сили в'язкого тертя, які гальмують обертання, компенсуються інтенсифікацією закрутки при переміщенні периферійних шарів, які обертаються повільно, до центру вихору завдяки поздовжньому розтягуванню. Аналіз цього механізму дозволив розробити порівняно просту модель вихрових структур, в якій сили в'язкого тертя і осьове розтягування вважаються нескінченно малими. При таких припущеннях можна використовувати рівняння руху ідеальної рідини в змінних «функція струму – завихренність». Показано, що при деяких припущеннях ці рівняння приймають вигляд хвильового рівняння, а граничними умовами є умова рівності нулю функції струму на твердих стінках потоку. Отримані рішення даного хвильового рівняння описують такі окремі випадки: вихори Гертлера між циліндрами, що обертаються, вторинні течії в трубі з квадратним поперечним перерізом, закручена течія в круглій трубі, парний вихор після повороту труби. Фізичний сенс більш складних рішень хвильового рівняння став зрозумілим порівняно недавно. Дуже схожі структури виявлені в експериментальних дослідженнях шляхом ортогонального розкладання (POD) поля турбулентних пульсацій. Це може означати, що базисні функції в POD відповідають когерентним структурам, реально виникають в потоці. Отримані результати свідчать на користь гіпотези, що вторинні течії і когерентні структури мають спільну природу. Рішення, отримані в даній роботі, можуть використовуватися при обробці експерименту в якості власних функцій для методу ортогонального розкладання. Крім того, вони можуть використовуватися при прямому чисельному моделюванні (DNS) турбулентних течій.

Ключові слова: *Вторинні течії; VLSM; Гогерентні структури; Метод ортогонального розкладання; Власні функції*

Література

1. **Nikuradze J.** Turbulente Strömungen in nicht kreisformigen Rohren // Ing.-Archiv. – 1930. – B. 1. – S. 306-332.
2. **Прандтль Л.** Гидроаэромеханика. – М.: Изд-во иностр. лит., 1951. – 576 с.
3. **Шлихтинг Г.** Теория пограничного слоя. – М.: Наука, 1974. – 712 с.
4. **Лойцянский Л. Г.** Механика жидкости и газа. – М.: Наука, 1987. – 840 с.
5. **Сурков С. В.** Хвильова модель вторинних течій в призматичних каналах // Тр. Одес. політехн. ун-ту. – 2002. – Вип. 2 (18). – С. 184-188.
6. **Сурков С. В.** Вторинні течії в каналах з круглим і кільцевим поперечним перерізом // Тр. Одес. політехн. ун-ту. – 2003. – Вип. 1 (19). – С. 14-18.
7. **Hellström L. H. O., Smits A. J.** The energetic motions in turbulent pipe flow // Physics of Fluids. – 2014. – 26, 125102. DOI: 10.1063/1.4902436
8. **Hellström L. H. O., Sinha A., Smits A. J.** Visualizing the very-large-scale motions in turbulent pipe flow // Physics of Fluids. – 2011. – 23, 011703. DOI: 10.1063/1.3533016
9. **Monty J. P., Stewart J. A., Williams R. C., Chong M. S.** Large-scale features in turbulent pipe and channel flows // Journal of Fluid Mechanics. – 2007. – 589, 147. DOI: 10.1017/S002211200700777X
10. **Baltzer J. R., Adrian R. J., Wu X.** Structural organization of large and very large scales in turbulent pipe flow simulation // Journal of Fluid Mechanics. – 2013. – Vol. 720, P. 236–279.
DOI: 10.1017/jfm.2012.642
11. **Dennis D. J. C., Sogaro F. M.** Distinct organizational states of fully-developed turbulent pipe flow //

Physical Review Letters. – 2014. – 113, 234501. DOI: 10.1103/PhysRevLett.113.234501

12**. Hellström L. H. O., Ganapathisubramani B., Smits A. J.** Coherent structures in transitional pipe flow // Physical Review Fluids. – 2016. – 1, 024403. DOI: 10.1103/PhysRevFluids.1.024403.

13. **Сурков С. В.** Комп'ютерна візуалізація плоских течій нестисливої рідини // Тр. Одес. політехн. ун-ту. – 2004. – Вип. 1 (21). – С. 205-208.

14. **Арсірій Е.А., Арсірій В.А., Василевська А.П.** Аналіз зображень гідродинамічних потоків за допомогою оцінки параметрів вихрових хвильових структур // Тр. Одес. полі-техн. ун-ту. – Одеса, 2005. – Вип. 1 (23). – С. 107-111.

15. **Arsiri V., Kravchenko O.** Reconstruction of turbomachines on the basis of the flow structure visual diagnostics // International Journal of Mechanics and Mechanical Engineering. – 2018. – Vol. 22. – No. 2. – P. 405-414. ISSN: 1428-151

16. **Matin R., Hellström L. H. O., Hernández-García A., Mathiesen J., Smits A. J.** Coherent structures in turbulent square duct flow // International Journal of Heat and Fluid Flow. – 2018. – Vol. 74, P. 144-153. DOI: 10.1016/j.ijheatfluidflow.2018.08.007

17. **Коренев Б. Г.** Некоторые задачи теории упругости и теплопроводности, решаемые в беселевых функциях. – М.: Физматгиз, 1960. – 460 с.

18. **Сурков С.В., Горбатенко Е.А.** Кінематичні властивості двопараметричних вихрових течій // Тр. Одес. політехн. ун-ту. – 2009. – Вип. 1 (31). – С. 139-142.

Отримана в редакції 27.09.2019, прийнята до друку 03.12.2019